μ_x boosted-bottom-jet tagging and Z' boson searches

Keith Pedersen[*] and Zack Sullivan[†]

Department of Physics, Illinois Institute of Technology, Chicago, Illinois 60616-3793, USA
(Received 18 November 2015; published 14 January 2016)

We present a new technique for tagging heavy-flavor jets with $p_T > 500$ GeV called "μ_x tagging." Current track-based methods of b-jet tagging lose efficiency and experience a large rise in fake rate in the boosted regime. Using muons from B hadron decay, we combine angular information and jet substructure to tag b jets, c jets, light jets, and "light-heavy" jets (those containing B hadrons from gluon splitting). We find tagging efficiencies of $\epsilon_b = 14\%$, $\epsilon_c = 6.5\%$, $\epsilon_{\text{light-light}} = 0.14\%$, and $\epsilon_{\text{light-heavy}} = 0.5\%$, respectively, that are nearly independent of transverse momentum at high energy. We demonstrate the usefulness of this new scheme by examining the discovery potential for multi-TeV leptophobic Z' bosons in the boosted-b-tagged dijet channel at the Large Hadron Collider.

I. INTRODUCTION

Searches for new narrow massive vector current particles, generally called Z' or W' bosons, are a main focus of the exotics groups in experiments at the Large Hadron Collider (LHC). These particles arise in many extensions of the standard model (SM), such as the sequential standard model [1], broken $\text{SU}(2)_L \times \text{SU}(2)_R$ symmetry [2–4], grand unified models [5–7], Kaluza-Klein excitations in models of extra dimensions [8,9], noncommuting extended technicolor [10], general extended symmetries [11,12], and more.

Using 8 TeV LHC data, the ATLAS [13] and CMS [14] collaborations set bounds on many types of Z' bosons that decay to dileptons below around 2.9 TeV. A more challenging search is for leptophobic gauge bosons, such as a top-color Z' boson, which is excluded up to 2.4 TeV [15–17], or a right-handed W' boson, which is excluded for SM-like couplings up to 1.9 TeV [18,19]. This latter boson is most strongly constrained by the $W' \to tb$ final state [20,21].

Flavor tagging such states becomes challenging in searches for vector boson resonances above 1.5 TeV, where dijet signals contain boosted-top jets [22–30] and boosted-bottom jets [21,31,32]. For example, the systematic uncertainties in b-tagging efficiency and fake rates dominate the current $W' \to tb$ limits, and have so far closed the $Z' \to b\bar{b}$ searches from consideration. This is evident in the ATLAS W' searches [18,33], which found a 35% uncertainty in the b-jet tagging efficiency for jets with p_T above 500 GeV (i.e. $M_{W'} \gtrsim 1$ TeV). This is mainly driven by a lack of clean samples of high-p_T b jets tagged with a complementary method, which are necessary to cross-check the signal/background efficiencies of the b tags [34–36]. Most concerning is the dramatic rise of the b-tagging fake rate

for jets initiated by light quarks as jet transverse momentum $p_T \to \mathcal{O}(\text{TeV})$ [37]. For instance, a CMS search for exotic resonances above 1.2 TeV encountered fake rates above 10% per jet [38].

This paper proposes an improvement to the *boosted-bottom-jet tag* first proposed in Ref. [21]. Here, the focus is on b quarks which are themselves highly boosted, instead of boosted topologies which contain bottom quarks (e.g., boosted $t \to Wb$ or $H \to b\bar{b}$). In Sec. II we explain why existing tagging methods are insufficient at high energies, and then derive from first principles a muon-based tag we call μ_x boosted-bottom-jet tagging. In Sec. III we present the μ_x tagging efficiencies for bottom and charm flavored jets, along with small light-jet fake rates, using a detailed simulation based on the ATLAS detector.

In order to determine the efficacy of this μ_x tag for new physics searches, we perform a full signal and background study for a leptophobic Z' boson [11,12]. This model assumes a flavor-independent Z'_B gauge coupling to SM quarks

$$\mathcal{L} = \frac{g_B}{6} Z'_{B\mu} \bar{q} \gamma^\mu q, \tag{1}$$

and demonstrates the power of our new boosted-bottom tag. We conclude in Sec. V with a discussion of other searches for physics beyond the standard model that this tag enables, and experimental information that could further improve the fake rejection for our algorithm.

II. TAGGING A HEAVY-FLAVORED JET

Heavy-quark (b or c) initiated jets shower and hadronize in a manner that is distinct from light parton (d, u, s, or g) initiated jets. The large masses of the heavy quarks ($m \gtrsim \Lambda_{\text{QCD}}$) cause their fragmentation functions to peak near $z = 1$. Thus, b and c quarks tend to retain their momentum during fragmentation [39], spawning heavy hadrons which carry a large fraction of their jet's

---
[*]kpeders1@hawk.iit.edu
[†]Zack.Sullivan@IIT.edu

014014-1

momentum. These hadrons have long lifetimes [$c\tau(B/D)\approx$ $\mathcal{O}(10^{-4}$ m)], and the decay daughters of even moderately boosted b/c hadrons will point back to secondary vertices (SV) whose impact parameters (IP) are far enough from the primary vertex to be resolved, but close enough to distinguish them from other meta-stable particles (e.g. $c\tau(K_S^0) = 3 \times 10^{-1}$ m). Additionally, the significant rate of semileptonic decay of b/c hadrons [$\mathcal{B}(X_{b/c} \to l\nu_l Y) \approx 0.1$ for each $l \in \{e, \mu\}$] enriches their jets with energetic leptons. Since bottom hadrons decay primarily to charm hadrons, b jets have twice the probability of c jets to contain leptons.

A. Challenges for existing b tags

Modern b-tagging algorithms are essentially track-based tags that search for evidence of a secondary vertex [40,41]. While they frequently use neural nets and multiple inputs, their efficiencies are predominantly determined by the impact parameter of a jet's tracks and the mass of its reconstructed SV. Although light jets also contain secondary vertices (e.g. K_S^0/Λ decay or material interaction [42]), this background is largely reducible for jets with $p_T < 300$ GeV, giving track tags high b jet efficiency (50–80%) and light jet fake rates of $\mathcal{O}(1\%)$. Above $p_T = 300$ GeV, the increasingly boosted nature of the jet makes track-tagging difficult. Boosted tracks bend less, and are thus harder to constrain and more sensitive to tracker resolution and alignment.

These problems are exacerbated in boosted heavy-flavor jets, where the primary hadron can decay *after* traversing one or more pixel layers, making it difficult or impossible for its daughters to produce the "high purity" tracks needed by most SV tagging algorithms. Additionally, if these collimated daughters strike *adjacent* pixels, they can create a "merged cluster" which also hinders reconstruction [41,43]. These problems are well exemplified by Fig. 12 of Ref. [44], where the light-jet fake rate of the "track counting high purity" algorithm increases 100-fold as jet p_T increases from 100 GeV to 1 TeV.

Another component of current b-tagging algorithms is p_T^{rel} tagging, which measures the momentum of leptons transverse to the centroid of their jet. Compared to light hadrons, heavy hadrons have a larger mass and carry a larger fraction of their jet's momentum; thus, leptons produced by heavy hadrons will have more energy and will arrive at wider angles inside the jet. These effects conspire to produce larger values of p_T^{rel} [44,45]. Since electrons are difficult to identify inside jets, p_T^{rel} tagging generally utilizes only muons. In ATLAS and CMS, muon p_T^{rel} tags give $\sim 10\%$ b jet efficiency and a light jet rejection (inverse tagging efficiency) of about 300 [45]. However, once jet p_T exceeds about 140 GeV, the underlying boost makes p_T^{rel} distributions for heavy and light jets nearly indistinguishable [36], precluding the tag.

B. The μ_x boosted-b tag

The failure of existing tagging methods to adequately reject high-p_T light jets is a problem. For track tagging, it is essentially a problem of detector resolution, so any improvements will likely involve novel utilization of the hardware and track observables. For p_T^{rel} tagging it is potentially a problem of definition; p_T^{rel} dilutes a well measured muon angle with a more poorly measured muon energy. This drove the development of the "boosted-bottom tag" [21], a purely angular tag on jets containing muons within $\Delta R = 0.1$ of their centroid. This tag achieves nearly ideal signal efficiency (given the muonic branching fraction), but suffers from a continuous rise with energy in light jet fake rate. Since the centroid of an *entire* jet is not necessarily aligned with the B hadron's decay, and the boost cone of muon emission should tighten as the boost increases, b jet decay should be reexamined in the context of jet substructure. This will provide the basis for a new heavy-flavor tag, which we dub the "μ_x boosted-b tag".

1. Theory of the μ_x tag

Consider a jet containing a B meson that decays semi-muonically. In the decay's center-of-momentum (CM) frame, the muon is emitted with speed $\beta_{\mu,\text{cm}}$ and angle θ_{cm} with respect to the boost axis (see Fig. 1). In the lab frame, the B meson's decay products are boosted (by γ_B) into a *subjet* with a hadronic "core" (which is typically a charm hadron) with four-momentum

$$p_{\text{subjet}} = p_{\text{core}} + p_\mu + p_{\nu_\mu}, \qquad (2)$$
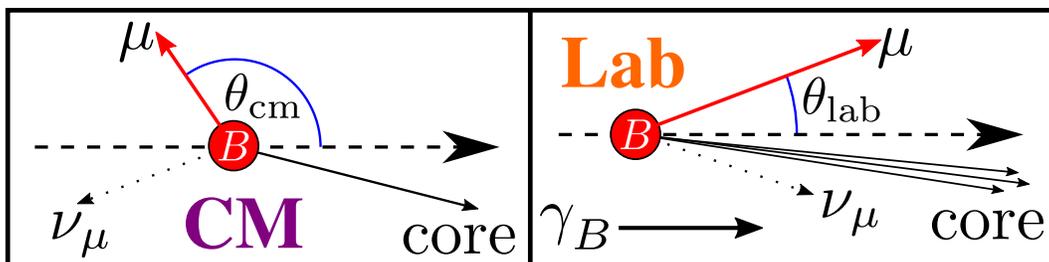
FIG. 1. Nomenclature for the center-of-momentum frame and boosted lab frame.

and the muon now makes the angle θ_{lab} with the B meson's direction.

Using basic kinematics, we can define a lab frame observable

$$x \equiv \gamma_B \tan(\theta_{\text{lab}}) = \frac{\sin(\theta_{\text{cm}})}{\kappa + \cos(\theta_{\text{cm}})}, \qquad (3)$$

where $\kappa \equiv \beta_B/\beta_{\mu,\text{cm}}$. While κ depends on the boost of the muon in the CM frame—which is generally not measurable—x itself has almost no dependence on κ when the system is sufficiently boosted ($\gamma_B \gg \gamma_{\mu,\text{cm}} \gtrsim 3$), as $\kappa \to 1$ in this limit. Fortuitously, the kinematics of both B meson decay and the jets of interest (jet $p_T > 300$ GeV) ensure this condition, giving lab frame muons from boosted B meson decay a nearly universal x distribution.

Assuming isotropic CM emission ($dN/d\Omega = \frac{1}{4\pi}$), the differential muon count N is

$$\frac{dN}{d\theta_{\text{cm}}} = \frac{1}{2}\sin(\theta_{\text{cm}}). \qquad (4)$$

When $\kappa \geq 1$, dN/dx can be written in the lab frame as

$$\frac{dN}{dx} = \frac{2x}{(x^2 + 1)^2} K(x, \kappa), \qquad (5)$$

where

$$K(x, \kappa) = \begin{cases} \frac{(1+\kappa^2)+x^2(1-\kappa^2)}{2\sqrt{1+x^2(1-\kappa^2)}} & 0 \leq x \leq 1/\sqrt{\kappa^2 - 1} \\ 0 & \text{everywhere else} \end{cases}. \qquad (6)$$

Here, $K(x, \kappa)$ enforces the boundary of the boost cone; i.e., when $\gamma_B \gg \gamma_{\mu,\text{cm}}$, the maximum value of x which a lab frame muon can achieve is $x = \sqrt{\gamma_{\mu,\text{cm}}^2 - 1}$.

As $K(x, \kappa) \to 1$ in the boosted limit ($\kappa = 1$), the muon distribution in x approaches a universal shape $2x/(x^2 + 1)^2$. We see the approach to this limit in Fig. 2, where the distribution of muon count vs. x is shown
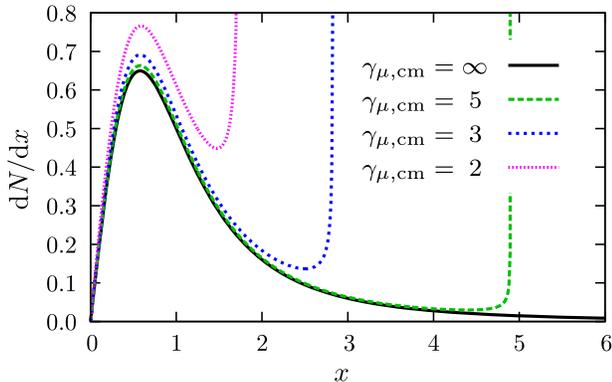
FIG. 2. Theoretical muon distribution dN/dx vs. x in the lab frame (with $\beta_B \to 1$) for various $\gamma_{\mu,\text{cm}}$.

for several muon boosts $\gamma_{\mu,\text{cm}}$. Since the typical muon boost in the CM frame $\gamma_{\mu,\text{cm}} > 3$, where deviations from the universal shape are small, the dN/dx of a typical muon is well represented by the boosted limit. This makes this universal shape useful for identifying muons from a boosted decay.

Assuming that all muons follow the universal shape, we calculate the largest value of x which confines a fraction ρ of lab frame muons (i.e. the inverse cumulative distribution),

$$x_\rho = \sqrt{\frac{\rho}{1 - \rho}}. \qquad (7)$$

We define a cut $x_{\text{max}} = x_{90\%}$ which accepts 90% of muons compatible with boosted B hadron decay. In addition, we use the hard fragmentation of b quarks to motivate a cut on the p_T fraction of the B hadron subjet to the total jet p_T

$$f_{\text{subjet}} \equiv \frac{p_{T,\text{subjet}}}{p_{T,\text{jet}}} \geq 0.5. \qquad (8)$$

These two cuts ($x \leq x_{\text{max}}$ and $f_{\text{subjet}} \geq f_{\text{subjet}}^{\text{min}}$) define the μ_x boosted-bottom-jet tag.

2. Reconstructing p_{subjet} and measuring x

Although x is defined in terms of an isolated decay of a bottom hadron, p_{subjet} will overlap other energy in the jet. Furthermore, half of a b jet's semimuonic decays come from charm hadrons. Therefore, it is not possible to measure γ_B—only γ_{subjet}. In spite of this limitation, we will see that it is still possible to reconstruct a meaningful x.

First, jets are clustered using the anti-k_T algorithm and a radius parameter $R = 0.4$. Muons are allowed to participate in jet clustering, which lets hard muons seed jet formation. Candidates for μ_x tagging must contain a *taggable* muon ($p_{T,\mu} \geq 10$ GeV) to ensure good muon reconstruction. While a taggable muon's associated neutrino is inevitably lost, most of the muon and neutrino momentum comes from their shared boost, making the muon an acceptable neutrino analog. We use the simplest choice: $p_{\nu_\mu} = p_\mu$.

A jet's internal list of candidate cores is obtained by reclustering the jet with the anti-k_T algorithm using $R_{\text{core}} = 0.04$; this radius is designed to localize the core to a 3×3 grid, based on the fixed width w of the calorimeter towers ($\sqrt{2}w < R_{\text{core}} < 2w$). All jet constituents are used during reclustering (allowing taggable muons to seed core formation) *except* towers failing a cut on jet p_T fraction (we choose $f_{\text{tower}}^{\text{min}} = 0.05$); this reduces the core's sensitivity to pileup, the underlying event, and soft QCD. Since the calorimeter granularity produces an ill-measured core mass, we fix the mass of each core candidate to a charm hadron mass $m_{\text{core}} = 2$ GeV. We identify the "correct" core as the candidate which brings $\sqrt{p_{\text{subjet}}^2}$ closest to

m_B, the nominal mass of the b hadron admixture (we choose $m_B = 5.3$ GeV).

Given our neutrino strategy ($p_{\nu_\mu} = p_\mu$), we can study the value of x that will be observed for an *arbitrary* muon-associated subjet (which *could* be the remnants of a B hadron, but could also be a random association of jet constituents). Such a subjet can be fully described using three lab frame observables: γ_{core} (the energy of the core), $\lambda = 2E_\mu/E_{\text{core}}$ (the energy of the muon, relative to the core), and ξ (the lab-frame angle between the muon and the *core*). Assuming that both the muon and the core are ultrarelativistic in the lab frame (i.e. $\beta \to 1$),

$$x(\xi) \approx \underbrace{\gamma_{\text{core}} \frac{1+\lambda}{\sqrt{1 + 2\lambda\gamma_{\text{core}}^2[1 - \cos(\xi)]}}}_{\gamma_{\text{subjet}}} \underbrace{\frac{\sin(\xi)}{\cos(\xi) + \lambda}}_{\tan(\theta_{\text{lab}})}, \quad (9)$$

where the square root term scales m_{core} to the larger m_{subjet}. This form reveals two distinct ξ regimes, visible in Fig. 3. When ξ is vanishingly small, $x(\xi) \approx \gamma_{\text{core}} \cdot \xi$. For intermediate ξ (large enough to dominate m_{subjet}, but small enough that $\tan(\theta_{\text{lab}}) \approx \frac{\xi}{1+\lambda}$), $x(\xi)$ flattens into a plateau at $x \approx 1/\sqrt{\lambda}$.

The x plateau exists because, as ξ rises, every increase in $\tan(\theta_{\text{lab}})$ is balanced by an increase in m_{subjet}. Once $m_{\text{subjet}} \gg m_B$, the reconstructed subjet is no longer consistent with a B hadron decay. This requires limiting m_{subjet} (we choose $m_{\text{subjet}}^{\text{max}} = 12$ GeV), which forces the x of poorly reconstructed (or fake) subjets to abruptly return to a nearly linear ξ dependence. This discontinuity is visible in Fig. 3. When the plateau is below x_{max}, the maximum taggable ξ is

$$\xi_{\text{max}}^{\text{hard}} \approx \frac{x_{\text{max}}}{\gamma_{\text{core}}} \left(\frac{m_{\text{subjet}}^{\text{max}}}{m_{\text{core}}}\right). \quad (10)$$

Thus, for *hard* muons ($\lambda \geq x_{\text{max}}^{-2}$), x_{max} is a purely angular cut which scales inversely proportional to the energy of the

core, with no additional dependence on the energy of the muon. On the other hand, when the plateau is above x_{max},

$$\xi_{\text{max}}^{\text{soft}} \approx \frac{x_{\text{max}}}{\gamma_{\text{core}}} \left(\frac{1}{\sqrt{1 - \lambda x_{\text{max}}^2}}\right). \quad (11)$$

So for *soft* muons ($\lambda < x_{\text{max}}^{-2}$), x_{max} is a much tighter angular cut which scales with the energy of both the core and the muon. But unless λ is near x_{max}^{-2} (the soft/hard muon boundary), $\xi_{\text{max}}^{\text{soft}}$ is only mildly sensitive to λ.

This means that x_{max} is effectively a dual angular cut: a very tight cut for soft muons, a looser cut for hard muons, and a quick transition region (as a function of muon energy) between the two classes. Thus, the μ_x tag depends primarily on well measured angles. For convenience, we summarize the parameters chosen for μ_x tagging in Table I.

III. μ_x TAGGING RESULTS

We extract the μ_x tagging efficiency for individual jets by simulating detector reconstruction for samples of flavored dijets. We generate all samples at $\sqrt{S} = 13$ TeV using MadGraph5 v2.2.3 [46] with CT14llo PDFs [47]. We use Pythia 8.210 [48,49] for all fragmentation, hadronization, and decay, using the default Pythia tune and PDF set for everything except pileup, for which we use the settings described in Table 7 of Ref. [50]. To allow in-flight muon production, we activate K_L^0, K^+ and π^+ decays.

We use FastJet 3.1.2 [51] to reconstruct jets, and a modified version of Delphes 3.2[52] to simulate the ATLAS detector at the LHC. Since the μ_x tag relies heavily on muon angle, with in-flight π^+/K^+ decays being a large source of muon background, we developed a custom module `AllParticlePropagator` to properly handle such decays. The module which implements μ_x tagging `MuXboostedBTagging` (available on GitHub [53]) can be used in conjunction with Delphes' default b tagging module `BTagging`. It is important to note that, until the most recent version of Delphes (3.3), the default Delphes cards define `BTagging` efficiencies which are *not accurate* at high p_T (e.g. light-jet fake rates are constant everywhere, and b/c jet efficiencies are constant for jets with $p_T \gtrsim 150$ GeV). The Delphes 3.3 efficiencies for 1–2 TeV jets are now 28%–14% for b-tags and 1%–2% for light jet fake rates. Our goal is to provide similar b-tagging efficiency with a factor of 10 improvement in fake rates.

Muon reconstruction efficiencies and p_T resolutions are taken from public ATLAS plots [54,55] for *stand-alone*

TABLE I. A summary of parameters chosen for μ_x boosted bottom jet tagging.

R	0.4	m_{core}	2 GeV	$p_{T,\mu}^{\text{min}}$	10 GeV
R_{core}	0.04	m_B	5.3 GeV	x_{max}	3 ($x_{90\%}$)
$f_{\text{tower}}^{\text{min}}$	0.05	$m_{\text{subjet}}^{\text{max}}$	12 GeV	$f_{\text{subjet}}^{\text{min}}$	0.5

FIG. 3. $x(\xi)$ for a subjet with $\gamma_{\text{core}} = 250$ and a hard muon ($\lambda = 1/7$).

muons (muons seen in the muon spectrometer (MS), but not necessarily the main tracker). Because the MS experiences limited punch-through, it can reconstruct muons with $p_T \geq 10$ GeV with high efficiency (95–99%), even inside boosted jets. Because we focus on the ATLAS MS, our results reflect the holes for detector services and support feet, which cause (i) a dip in muon reconstruction efficiency at $\eta = 0$ [56], precisely where the dijet $dN/d\eta$ distribution peaks, and (ii) 80% geometric acceptance of the Level-1 muon trigger in the barrel [57]. This latter restriction can be resolved by relying on jet triggers (jet p_T or event H_T) to select pertinent events, since μ_x tagging only works for high-p_T jets.

There are several sources of stand-alone muon background which we are unable to simulate: (i) cosmic muons, (ii) decay muons from particles produced in the calorimeter shower, (iii) fake muons from punch-through, and (iv) fake muons from noise. Nonetheless, since the μ_x tag is effectively a tight angular cut with a reasonably high $p_{T,\mu}$ threshold, we expect these backgrounds to be negligible compared to the light jet background which we simulate.

The direction of the core is extremely important in μ_x tagging, and tracks would provide the best information. However, the core's intrinsic collimation hampers track reconstruction in a manner difficult to model in a fast detector simulation. As such, we build jets (and cores) solely from calorimeter towers and muons. The coarse granularity of the hadronic calorimeter (HCal) is mitigated by using the finer granularity of the EM calorimeter (ECal) to orient the combined tower ("ECal pointing"). This is implemented in Delphes' Calorimeter module by giving both ECal and HCal the segmentation of ATLAS's ECal Layer-2 ($\Delta\phi \times \Delta\eta = 0.025 \times 0.025$ in the barrel). To ensure that we are not overly sensitive to this resolution,

we also test a granularity twice as coarse (0.05×0.05), finding negligible degradation in the heavy jet tagging efficiency, with only a slight rise in light jet fake rate (1.2 times larger at $p_T = 600$ GeV, but dropping to no increase at 2.1 TeV).

A. Tagging efficiencies

To test the μ_x tag, we create ten 200 GeV wide samples of $b\bar{b}$, $c\bar{c}$, and $j\bar{j}$ ($j \in \{u, d, s, g\}$) spanning $p_T = 0.1$–2.1 TeV. We then find the efficiency to tag the top two jets (ranked by p_T) in each event. Since heavy hadrons from gluon splitting ($g \to b\bar{b}/c\bar{c}$) are an inevitable component of our light-jet sample, especially at high p_T, it is important to determine the extent to which this background can be reduced. We sort the light jet sample via the truth-level flavor of a taggable muon's primary hadronic precursor. This classifies each attempted tag as *light-heavy* (where the muon descends from a b/c hadron inside a jet initiated by a light parton) or *light-light* (where the muon's lineage is a purely light-flavored).

In Fig. 4 we show our predicted efficiencies for the four classes of μ_x tags. The solid lines represent the efficiencies without pileup, while the dotted lines show the efficiencies when a random number of pileup events (drawn from a Poisson distribution with $\mu = 40$) are added to each hard event. Since we do not utilize nonmuon tracking, and are working with TeV-scale jets, we do not attempt any pileup subtraction.

Each p_T bin in Fig. 4a sums over all available η_{jet}. When the boosted approximations are valid (jet $p_T \geq 300$ GeV), the efficiency to tag heavy jets is nearly flat versus p_T, while the efficiency to tag light jets decreases slightly. We find asymptotic tagging efficiencies of $\epsilon_b = 14\%$, $\epsilon_c = 6.5\%$, $\epsilon_{\text{light-light}} = 0.14\%$, and $\epsilon_{\text{light-heavy}} = 0.5\%$, respectively. This light-light rejection provides us the full factor of 10
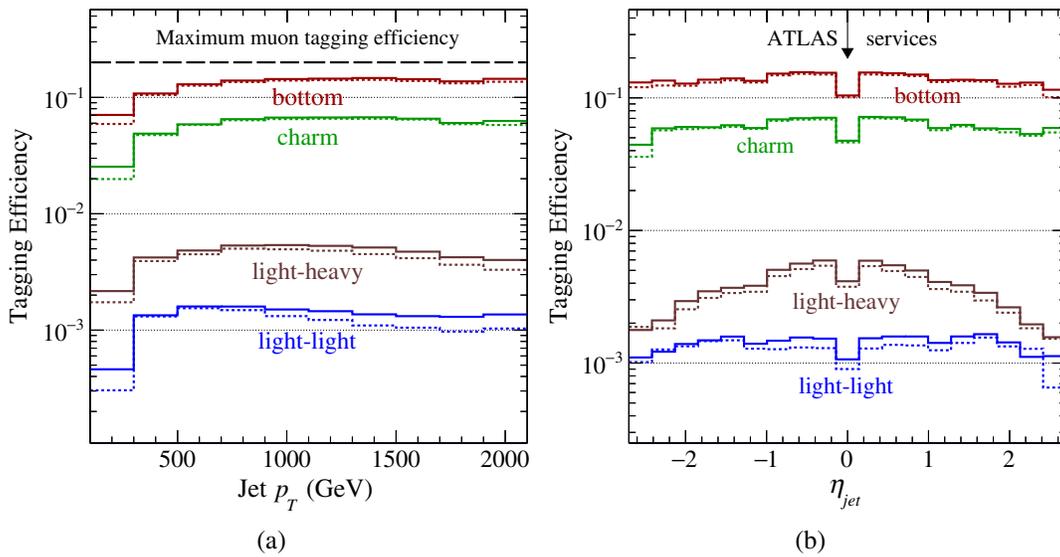
FIG. 4. μ_x tagging efficiency vs. (a) jet p_T and (b) η_{jet}.

improvement over existing algorithms. At low-p_T (where B hadrons are no longer strongly boosted and track tagging is superior) all μ_x efficiencies plummet, although the relative rates remain approximately the same. Notice that pileup actually *improves* the performance of μ_x tagging above 1 TeV, causing almost no degradation in heavy-jet efficiencies, but a significant drop in light-jet efficiency. This is a consequence of the increased probability for light jets to reconstruct a subjet with a low fraction of total jet energy, thereby failing the cut on f_{subjet}.

Since the μ_x tag is not effective at low p_T, each η_{jet} bin in Fig. 4b requires $p_T \geq 300$ GeV. We can see that both heavy and light-light jet efficiencies are flat with η_{jet}. The light-heavy efficiency decreases significantly with $|\eta_{\text{jet}}|$, indicating a rising rejection of heavy hadron background from gluon splitting. This suggests the intriguing possibility that the $g \rightarrow b\bar{b}$ contribution to b jets could be extracted from data, and used to calibrate the Monte Carlo event generators for highly boosted jets.

The underlying physics of μ_x tagging is evident in Fig. 5. The x distribution for *bottom* jets peaks at $x \approx 0.8$ (versus dN/dx, which peaks around $x \approx 0.6$). This is due to a convolution of direct-b and secondary-c decay, since c hadron decays peak around $x = 1$ (Fig. 5b). In both

heavy-jet classes, the f_{subjet} distributions favor subjets carrying nearly all of their jet's momentum.

The x distribution for *light-light* jets with sufficient f_{subjet} peaks to the right of x_{max}, whereas muons with taggable x tend to be clustered into overly soft subjets. Since *light-heavy* jets contain heavy hadrons, their high-f_{subjet} muons should (and do) have b-like values of x. However, since the initial jet momentum must be shared between a pair of heavy hadrons, many light-heavy muons with taggable x fail $f_{\text{subjet}}^{\text{min}}$, which suppresses this background.

IV. LEPTOPHOBIC Z'

A simple extension of the standard model involves the addition of a broken $U(1)'$ symmetry mediated by a heavy neutral Z' boson. If the new symmetry is associated with baryon number B, one would not expect to see a dilepton signal, since only SM quarks would be charged. To cancel anomalies, this $U(1)'_B$ should couple to vectorlike quarks, and come with at least one scalar field whose vacuum expectation value breaks the symmetry [11,12]. Assuming the vectorlike quarks are kinematically inaccessible at the LHC, a flavor-independent Z'_B gauge coupling to SM quarks [11]
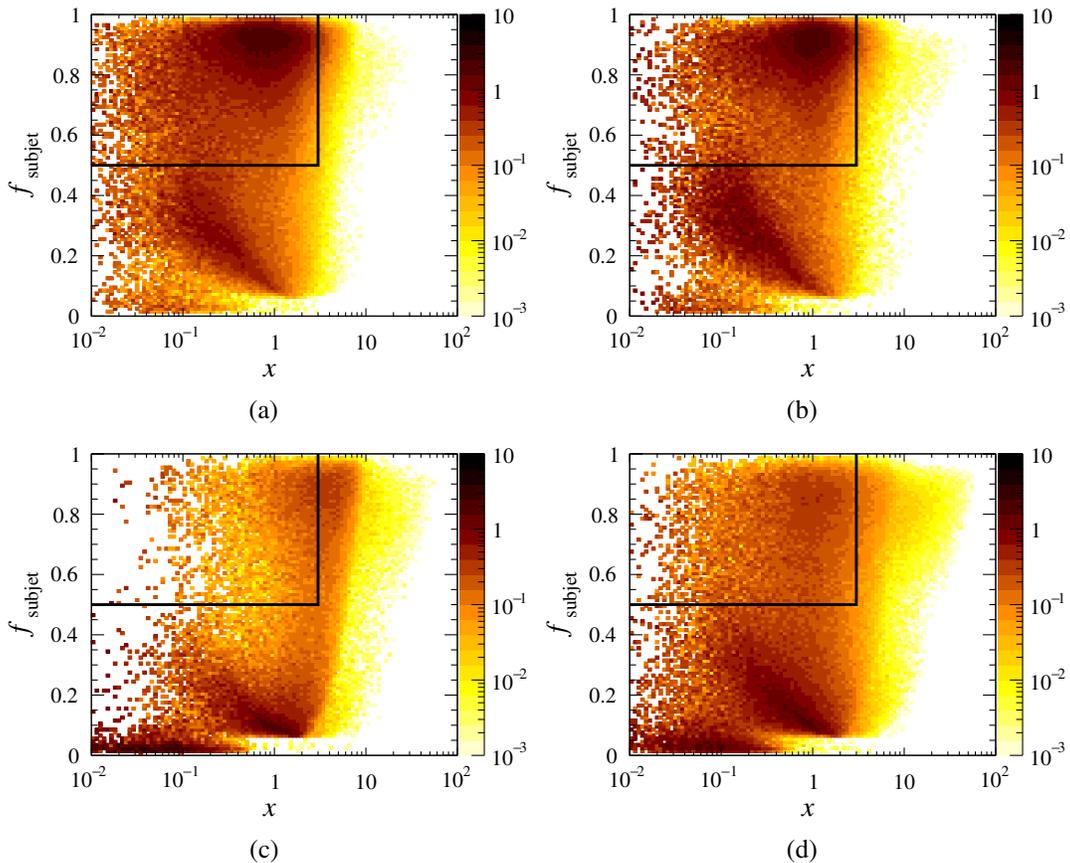
FIG. 5. Density of reconstructed candidate tags with $\mu = 40$ pileup events as a function of f_{subjet} vs. x (summing over all p_T and η_{jet} bins) for (a) bottom, (b) charm, (c) light-light, and (d) light-heavy jets.

$$\mathcal{L} = \frac{g_B}{6} Z'_{B\mu} \bar{q} \gamma^\mu q \qquad (12)$$

might lead to dijets being the only detectable signature at the LHC of this new physics.

We would expect the purity of a dijet Z' signal to be very low, since QCD production of dijets has an enormous cross section. This is where μ_x tagging is useful, as the rejection of light-jet fakes seen in Sec. III A is $\mathcal{O}(10^3)$. To validate our new boosted-b tag, we simulate a search for a narrow Z'_B peak above the dijet background at Run II of the LHC (i.e., looking for an excess in the $d\sigma/dm_{jj}$). We examine the experimental reach in two dijet samples: 2-tag and 1-tag inclusive (where N-tag requires at least N of the top two p_T-ranked jets to be μ_x-tagged).

We model Z'_B production for a variety of $M_{Z'_B}$ spanning 1–4 TeV, using $pp \to Z'_B \to b\bar{b}/c\bar{c}(+j)$. The optional light-jet radiation slightly enhances the overall Z'_B cross-section, but is mostly useful to improve the differential jet distribution via MLM jet matching [58] in both MadGraph and Pythia (in "shower-kt" mode [59], using a matching scale of $M_{Z'_B}/20$). As before, all reconstruction is performed using our modified Delphes code.

The relevant background is pure QCD, as no other SM processes contain competing cross-sections. Both 2-tag and 1-tag backgrounds contain $pp \to b\bar{b}/c\bar{c}/j\bar{j}(+j)$. The 1-tag background also includes a large contribution from $jq_h \to jq_h(+j)$ (a heavy quark scattering off a light parton). To obtain good tagging statistics, multiple background sets are generated, using identical matching parameters as their corresponding signal set.

The minuscule light-jet tagging efficiency forces us to estimate the *second* tag for the 2-tag light-dijet background sample by using our fit to the light-jet efficiency from Sec. III A as a function of jet p_T and η_{jet}. When exactly one leading jet is tagged, we estimate the probability ϵ_l to tag the other jet, then reweight the event by a factor of $\frac{\epsilon_l}{2(1-\epsilon_l)}$. When both leading jets are tagged, the event is discarded, otherwise it would be double counted by this method.

Additional cuts for our analysis include a requirement that the pseudorapidity between jets is small $|\Delta\eta_{jj}| \leq 1.5$ in order to suppress much of the t-channel dijet background. We also require $|\eta_{\text{jet}}| \leq 2.7$ to ensure that both jets fall within the muon spectrometer. While we considered including the effects of higher order final state radiation in our mass reconstruction, we find that adding a hard third jet to the dijet system causes an unacceptable hardening of the QCD continuum. Not including this radiation, combined with the estimation of hard neutrino momenta inherent to μ_x tagging, decreases the mass resolution of the intrinsically narrow Z'_B bosons of this model ($\Gamma_{Z'} = \frac{1}{6}\alpha_B(1 + \alpha_s/\pi)M_{Z'}$). Hence, we require a rather wide mass window ($[0.85, 1.25] \times M_{Z'_B}$) to capture most of the signal.

The signal and backgrounds for a 5σ discovery of a $M_{Z'_B} = 2.5$ TeV Z'_B boson, using our cuts for the 2-tag and 1-tag analyses, can be seen in Fig. 6 for 100 fb^{-1} of integrated luminosity at the 13 TeV LHC. The signal to background ratio $S/B = 1/2$ for the 2-tag sample, indicating an excellent purity. The 1-tag sample has $S/B = 1/12$, still acceptable given the factor of 12 more signal events that would appear in the sample. The peak in the 1-tag sample is slightly narrower than the 2-tag sample because only one neutrino is estimated in the boosted jet decay.

In Fig. 7 we depict the estimated discovery potential for the 2- and 1-tag analyses, along with the 1-tag 95% confidence level (C.L.) exclusion limits, for the LHC Run II with the scheduled luminosity of 100 fb^{-1}. Comparing our results to the existing exclusions limits presented in Fig. 1 of Ref. [11], our 2-tag discovery reach is about 500 GeV higher in mass for large g_B, and is right at the limit for smaller g_B. Not shown in the figure is the 95% C.L. exclusion limit for the 2-tag search, which is slightly better than the 5σ discovery reach in the 1-tag search. The 1-tag search dramatically improves the mass reach by ~ 1.5 TeV beyond the current limits at large g_B and, more importantly, can attain $g_B < 1$ below 2(3) TeV for discovery(exclusion).
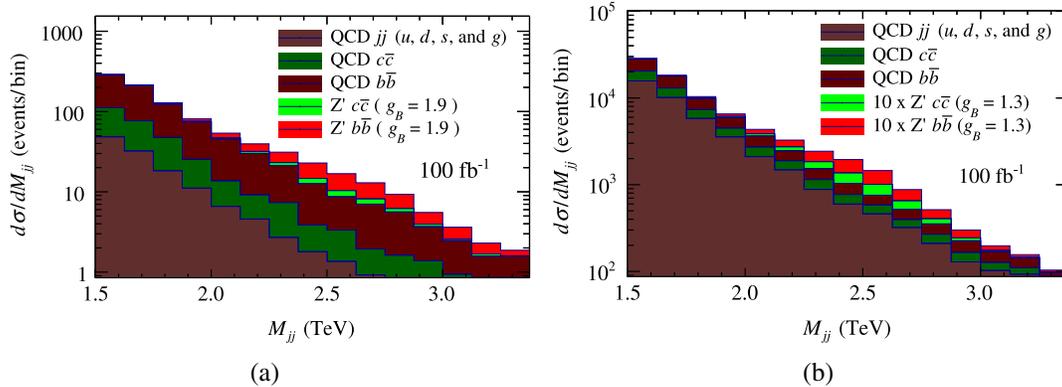
FIG. 6.   Events per bin expected for 5σ discovery of a $M_{Z'_B} = 2.5$ TeV signal, and backgrounds, in the (a) 2-tag and (b) 1-tag analyses using 100 fb^{-1} of integrated luminosity at Run II of the LHC.
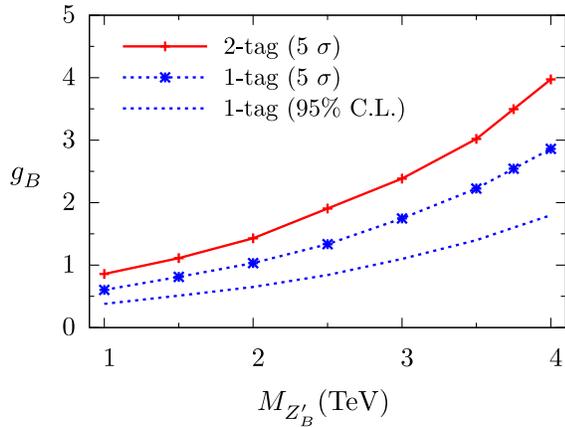
FIG. 7.   Estimated Run II (100 fb^{-1}) 5σ discovery potential and 95% confidence level exclusion limits for g_B vs. $M_{Z'_B}$ for the 2-tag and 1-tag analyses. 2-tag 95% C.L. exclusion reach (not shown) is comparable to the 1-tag discovery reach.

Hence, the μ_x boosted-bottom tag opens a new window into leptophobic Z' boson physics.

V. CONCLUSIONS

In this paper we derive and examine the efficacy of the new μ_x boosted-bottom-jet tag. The μ_x tag enables a new class of high purity searches for final states containing b jets in the decays of TeV-scale particles. In Sec. IV we propose the use of the μ_x boosted-bottom jet tag to discover a leptophobic Z' boson at the 13 TeV Run II of the LHC. We perform two analyses based on the number of μ_x boosted-b tags: a high purity analysis with two b tags, and an extended-reach analysis based on a one-tag inclusive sample. We find the potential for discovery of a Z'_B boson with universal coupling to quarks can be extended by 500–1000 GeV beyond existing 95% C.L. exclusion limits [11], or to a factor of two smaller coupling g_B.

The μ_x boosted-bottom-jet tag improves on the idea of using the angle between a muon from B hadron decay and the jet centroid proposed in Ref. [21]. By measuring the angle between the muon and the subjet inside the b-jet that is likely to contain the B hadron remnant, this "smart" angular cut (loose for hard muons, tight for soft muons, and scaling with the boost) obtains efficiencies to tag b-jets, c-jets, light-jets, and light-heavy jets (in which $g \to b\bar{b}$ produces real B hadrons) of $\epsilon_b = 14\%$, $\epsilon_c = 6.5\%$, $\epsilon_{\text{light-light}} = 0.14\%$, and $\epsilon_{\text{light-heavy}} = 0.5\%$, respectively. Since the light-light fake rate is a factor of 10 smaller than current b tag estimates [60], the μ_x boosted-b tag should greatly improve the uncertainties in the search for $W' \to t\bar{b}$ at ATLAS [18,33].

Several other applications exist for μ_x boosted-b tagging, such as the search for heavy Higgs bosons in general two Higgs doublet models with moderate $\tan(\beta)$ [61,62]. When boosted-bottom tagging is combined with boosted-top tagging, decays of heavy Higgs bosons should be accessible in the channels $pp \to \bar{b}tH^- \to \bar{b}t\bar{t}b$ and $pp \to b\bar{b}H/A \to b\bar{b}t\bar{t}$. Another important application of μ_x tagging is the use of the pseudorapidity-dependent fake rate from gluon splitting to provide an experimental handle to calibrate this contribution to jet showering at TeV energies.

While we derive the μ_x boosted-bottom-jet tag from basic kinematics in Sec. II, in this paper we examine its effectiveness at the LHC in the context of the ATLAS detector. This choice is driven by the public ATLAS stand-alone/nonisolated muon reconstruction capabilities as a function of p_T and η [55]. We ensure that our b tag is robust in a realistic detector environment by simulating ATLAS detector subsystems in Delphes, and establishing an insensitivity to the detector details. Given that the μ_x boosted-b tag is driven by physical principles, and not detector idiosyncrasies, we are confident it will work just as well with the CMS detector provided the nonisolated muons can be reconstructed.

Naturally, the μ_x tag will require experimental validation using heavy-flavor enriched and deficient control samples from CMS and ATLAS. A comparison of the μ_x tag to existing b tags around 500 GeV (the lowest energy with good efficiency overlap) will permit the extension of the μ_x tag to the highly boosted regime, where smaller uncertainties are sorely needed. The b jet efficiency could be extracted from $t\bar{t}$ events (~36% of which should contain a semi-muonic B decay). To calibrate the light-jet fake rate we suggest looking in a light-jet enriched dijet sample: where one jet lacks a muon and fails a "loose" track-based b tag, and the other jet contains a muon. This tag-and-probe method should enhance the purity of the already large cross section ratio $\sigma_{j\bar{j}}/\sigma_{b\bar{b}}$ by a factor of 5.

It is possible that additional improvements to the μ_x tag can be made using capabilities specific to a given experiment. For example, the final layer of the ATLAS inner detector has very fine ϕ resolution, while the first layer of the ATLAS ECal has excellent η resolution. Since the direction of the "core" subjet is more important than the properties of its charged constituents (track quantity, impact parameters, opening angles), it may be possible to interrogate the *global* nature of the core without attempting to reconstruct its individual tracks. Given enough angular resolution, a direct measurement of m_{core} could replace its manual constraint. This procedure is essentially an extension of CMS' particle flow algorithm to very boosted hadronic substructure.

We have described a new method for tagging boosted ($p_T > 500$ GeV) jets that contain heavy hadrons we call μ_x-tagging. This tag significantly improves the purity of b-tagging in the boosted regime, and will greatly extend the reach of searches for physics beyond the standard model. We conclude with the observation that while we have tuned

μ_x-tagging for boosted b jets, the underlying kinematics of heavy hadron decay is equally applicable to charm jets, and a retuning of parameters may provide an enhanced sensitivity to boosted-charm jet tagging.

[1] G. Altarelli, B. Mele, and M. Ruiz-Altaba, Searching for new heavy vector bosons in $p\bar{p}$ colliders, Z. Phys. C **45,** 109 (1989); **47,** 676(E) (1990).

[2] R. N. Mohapatra and J. C. Pati, Left-right gauge symmetry and an 'isoconjugate' model of CP violation, Phys. Rev. D **11,** 566 (1975).

[3] R. N. Mohapatra and J. C. Pati, A 'natural' left-right symmetry, Phys. Rev. D **11,** 2558 (1975).

[4] G. Senjanovic and R. N. Mohapatra, Exact left-right symmetry and spontaneous violation of parity, Phys. Rev. D **12,** 1502 (1975).

[5] M. Cvetic and J. C. Pati, $N = 1$ supergravity within the minimal left-right symmetric model, Phys. Lett. **135B,** 57 (1984).

[6] J. L. Hewett and T. G. Rizzo, Low-energy phenomenology of superstring inspired E(6) models, Phys. Rep. **183,** 193 (1989).

[7] A. Leike, The phenomenology of extra neutral gauge bosons, Phys. Rep. **317,** 143 (1999).

[8] L. Randall and R. Sundrum, A Large Mass Hierarchy from a Small Extra Dimension, Phys. Rev. Lett. **83,** 3370 (1999).

[9] L. Randall and R. Sundrum, An Alternative to Compactification, Phys. Rev. Lett. **83,** 4690 (1999).

[10] R. S. Chivukula, E. H. Simmons, and J. Terning, Limits on noncommuting extended technicolor, Phys. Rev. D **53,** 5258 (1996).

[11] B. A. Dobrescu and F. Yu, Coupling-mass mapping of dijet peak searches, Phys. Rev. D **88,** 035021 (2013); **90,** 079901 (E) (2014).

[12] B. A. Dobrescu, Leptophobic boson signals with leptons, jets and missing energy, arXiv:1506.04435.

[13] G. Aad *et al.* (ATLAS Collaboration), Search for high-mass dilepton resonances in pp collisions at $\sqrt{s} = 8$ TeV with the ATLAS detector, Phys. Rev. D **90,** 052005 (2014).

[14] V. Khachatryan *et al.* (CMS Collaboration), Search for physics beyond the standard model in dilepton mass spectra in proton-proton collisions at $\sqrt{s} = 8$ TeV, J. High Energy Phys. 04 (2015) 025.

[15] S. Chatrchyan *et al.* (CMS Collaboration), Searches for New Physics Using the $t\bar{t}$ Invariant Mass Distribution in pp Collisions at $\sqrt{s} = 8$ TeV, Phys. Rev. Lett. **111,** 211804 (2013); **112,** 119903(E) (2014).

[16] G. Aad *et al.* (ATLAS Collaboration), A search for $t\bar{t}$ resonances using lepton-plus-jets events in proton-proton collisions at $\sqrt{s} = 8$ TeV with the ATLAS detector, J. High Energy Phys. 08 (2015) 148.

[17] V. Khachatryan *et al.* (CMS Collaboration), Search for resonant ttbar production in proton-proton collisions at $\sqrt{s} = 8$ TeV, arXiv:1506.03062 [Phys. Rev. D (to be published)].

[18] G. Aad *et al.* (ATLAS Collaboration), Search for $W' \to t\bar{b}$ in the lepton plus jets final state in proton-proton collisions at a centre-of-mass energy of $\sqrt{s} = 8$ TeV with the ATLAS detector, Phys. Lett. B **743,** 235 (2015).

[19] S. Chatrchyan *et al.* (CMS Collaboration), Search for a W' boson decaying to a bottom quark and a top quark in pp collisions at $\sqrt{s} = 7$ TeV, Phys. Lett. B **718,** 1229 (2013).

[20] Z. Sullivan, Fully differential W' production and decay at next-to-leading order in QCD, Phys. Rev. D **66,** 075011 (2002).

[21] D. Duffty and Z. Sullivan, Searching for W' bosons through decays to boosted-top and boosted-bottom jets, Phys. Rev. D **90,** 015031 (2014).

[22] D. E. Kaplan, K. Rehermann, M. D. Schwartz, and B. Tweedie, Top Tagging: A Method for Identifying Boosted Hadronically Decaying Top Quarks, Phys. Rev. Lett. **101,** 142001 (2008).

[23] CMS Collaboration, Report No. CMS-PAS-JME-09-001.

[24] L. G. Almeida, S. J. Lee, G. Perez, I. Sung, and J. Virzi, Top jets at the LHC, Phys. Rev. D **79,** 074012 (2009).

[25] J. Thaler and K. Van Tilburg, Identifying boosted objects with N-subjettiness, J. High Energy Phys. 03 (2011) 015.

[26] C. Anders, C. Bernaciak, G. Kasieczka, T. Plehn, and T. Schell, Benchmarking an even better top tagger algorithm, Phys. Rev. D **89,** 074047 (2014).

[27] CMS Collaboration, Report No. CMS-PAS-JME-13-007.

[28] L. G. Almeida, M. Backovic, M. Cliche, S. J. Lee, and M. Perelstein, Playing tag with ANN: Boosted top identification with pattern recognition, J. High Energy Phys. 07 (2015) 086.

[29] G. Kasieczka, T. Plehn, T. Schell, T. Strebler, and G. P. Salam, Resonance searches with an updated top tagger, J. High Energy Phys. 06 (2015) 203.

[30] E. Usai (ATLAS and CMS Collaborations), Boosted top: Experimental tools overview, arXiv:1501.00900.

[31] CMS Collaboration, Report No. CMS-PAS-BTV-13-001.

[32] H. Bachacou *et al.* (ATLAS Collaboration), Report No. ATL-PHYS-PUB-2014-014.

[33] G. Aad *et al.* (ATLAS Collaboration), Search for $W' \to tb \to qqbb$ decays in pp collisions at $\sqrt{s} = 8$ TeV with the ATLAS detector, Eur. Phys. J. C **75,** 165 (2015).

[34] ATLAS Collaboration, Report No. ATLAS-CONF-2014-004.

[35] ATLAS Collaboration, Report No. ATLAS-CONF-2014-046.

[36] G. Aad *et al.* (ATLAS Collaboration), Report No. ATLAS-CONF-2011-089.

[37] G. Aad *et al.* (ATLAS Collaboration), Report No. ATL-PHYS-PUB-2014-014.

[38] V. Khachatryan *et al.* (CMS Collaboration), Search for resonances and quantum black holes using dijet mass spectra in proton-proton collisions at $\sqrt{s} = 8$ TeV, Phys. Rev. D **91**, 052009 (2015).

[39] M. Cacciari, Fragmentation functions of light and heavy quarks, CTEQ Summer School (1998), [http://users.phys .psu.edu/~cteq/schools/summer98/].

[40] G. Aad *et al.* (ATLAS Collaboration), Report No. ATLAS-CONF-2011-102.

[41] S. Chatrchyan *et al.* (CMS Collaboration), Identification of *b*-quark jets with the CMS experiment, J. Instrum. **8**, P04013 (2013).

[42] G. Aad *et al.* (ATLAS Collaboration), A study of the material in the ATLAS inner detector using secondary hadronic interactions, J. Instrum. **7**, P01013 (2012).

[43] G. Aad *et al.* (ATLAS Collaboration), A neural network clustering algorithm for the ATLAS silicon pixel detector, J. Instrum. **9**, P09009 (2014).

[44] S. Chatrchyan *et al.* (CMS Collaboration), Report No. CMS-PAS-BTV-09-001.

[45] H. Bachacou *et al.* (ATLAS Collaboration), Report No. ATL-PHYS-PUB-2009-021, ATL-COM-PHYS-2009-210.

[46] J. Alwall, R. Frederix, S. Frixione, V. Hirschi, F. Maltoni, O. Mattelaer, H.-S. Shao, T. Stelzer, P. Torrielli, and M. Zaro, The automated computation of tree-level and next-to-leading order differential cross sections, and their matching to parton shower simulations, J. High Energy Phys. 07 (2014) 079.

[47] S. Dulat *et al.*, The CT14 Global Analysis of Quantum Chromodynamics, arXiv:1506.07443.

[48] T. Sjostrand, S. Mrenna, and P. Z. Skands, PYTHIA 6.4 physics and manual, J. High Energy Phys. 05 (2006) 026.

[49] T. Sjostrand, S. Mrenna, and P. Z. Skands, A brief introduction to PYTHIA 8.1, Comput. Phys. Commun. **178**, 852 (2008).

[50] G. Aad *et al.* (ATLAS Collaboration), Reports No. ATL-PHYS-PUB-2011-009, No. ATL-COM-PHYS-2011-744.

[51] M. Cacciari, G. P. Salam, and G. Soyez, FastJet User Manual, Eur. Phys. J. C **72**, 1896 (2012).

[52] J. de Favereau, C. Delaere, P. Demin, A. Giammanco, V. Lemaître, A. Mertens, and M. Selvaggi (DELPHES 3 Collaboration), DELPHES 3, A modular framework for fast simulation of a generic collider experiment, J. High Energy Phys. 02 (2014) 057.

[53] K. Pedersen, https://github.com/keith-pedersen/delphes/ tree/MuXboostedBTagging.

[54] G. Aad *et al.* (ATLAS Collaboration), The ATLAS experiment at the CERN Large Hadron Collider, J. Instrum. **3**, P07007 (2008).

[55] G. Aad *et al.* (ATLAS Collaboration), https://twiki.cern.ch/ twiki/bin/view/AtlasPublic/ApprovedPlotsMuon.

[56] G. Aad *et al.* (ATLAS Collaboration), Measurement of the muon reconstruction performance of the ATLAS detector using 2011 and 2012 LHC protonproton collision data, Eur. Phys. J. C **74**, 3130 (2014).

[57] G. Aad *et al.* (ATLAS Collaboration), Performance of the ATLAS muon trigger in pp collisions at $\sqrt{s} = 8$ TeV, Eur. Phys. J. C **75**, 120 (2015).

[58] M. L. Mangano, M. Moretti, F. Piccinini, and M. Treccani, Matching matrix elements and shower evolution for top-quark production in hadronic collisions, J. High Energy Phys. 01 (2007) 013.

[59] J. Alwall, S. de Visscher, and F. Maltoni, QCD radiation in the production of heavy colored particles at the LHC, J. High Energy Phys. 02 (2009) 017.

[60] G. Aad *et al.* (ATLAS Collaboration), Report No. ATL-PHYS-PUB-2015-022.

[61] N. Craig, F. D'Eramo, P. Draper, S. Thomas, and H. Zhang, The hunt for the rest of the Higgs bosons, J. High Energy Phys. 06 (2015) 137.

[62] J. Hajer, Y. Y. Li, T. Liu, and J. F. H. Shiu, Heavy Higgs bosons at 14 TeV and 100 TeV, J. High Energy Phys. 11 (2015) 124.